Received: 23 October 2017 | Revised: 28 September 2018 | Accepted: 30 October 2018

DOI: 10.1111/mec.14964

ORIGINAL ARTICLE

WILEY MOLECULAR ECOLOGY

Reduced skin bacterial diversity correlates with increased pathogen infection intensity in an endangered amphibian host

Silas Ellison[1] | Roland A. Knapp[2] | Wesley Sparagon[3] | Andrea Swei[1] | Vance T. Vredenburg[1,4]

[1]Department of Biology, San Francisco State University, San Francisco, California

[2]Sierra Nevada Aquatic Research Laboratory, University of California, Mammoth Lakes, California

[3]Department of Biology, Whitman College, Walla Walla, Washington

[4]Museum of Vertebrate Zoology, University of California, Berkeley, California

Correspondence
Silas Ellison, Department of Biology, San Francisco State University, San Francisco, CA.
Email: silas.d.l.ellison@gmail.com

Present Address
Wesley Sparagon, Center for Microbial Oceanography: Research and Education, University of Hawaii at Manoa, Honolulu, Hawaii

Funding information
San Francisco State University Biology Department; California State University Program for Education and Research in Biotechnology; U.S. Forest Service Southern Nevada Public Lands Management Act, Grant/Award Number: 13-DG-11272170-002; American Museum of Natural History; National Science Foundation, Grant/Award Number: DEB-11202283 and NSF 1633948

Abstract

The fungal pathogen *Batrachochytrium dendrobatidis* (*Bd*) infects the skin of amphibians and has caused severe declines and extinctions of amphibians globally. In this study, we investigate the interaction between *Bd* and the bacterial skin microbiome of the endangered Sierra Nevada yellow-legged frog, *Rana sierrae*, using both culture-dependent and culture-independent methods. Samples were collected from two populations of *R. sierrae* that likely underwent *Bd* epizootics in the past, but that continue to persist with *Bd* in an enzootic disease state, and we address the hypothesis that such "persistent" populations are aided by mutualistic skin microbes. Our 16S rRNA metabarcoding data reveal that the skin microbiome of highly infected juvenile frogs is characterized by significantly reduced species richness and evenness, and by strikingly lower variation between individuals, compared to juveniles and adults with lower infection levels. Over 90% of DNA sequences from the skin microbiome of highly infected frogs were derived from bacteria in a single order, Burkholderiales, compared to just 54% in frogs with lower infection levels. In a culture-dependent *Bd* inhibition assay, the bacterial metabolites we evaluated all inhibited the growth of *Bd*. Together, these results illustrate the disruptive effects of *Bd* infection on host skin microbial community structure and dynamics, and suggest possible avenues for the development of anti-*Bd* probiotic treatments.

KEYWORDS
amphibian, *Batrachochytrium dendrobatidis*, chytridiomycosis, diversity, enzootic dynamics, microbiome

1 | INTRODUCTION

Emerging infectious diseases have increasingly become a threat to biodiversity (Daszak, Cunningham, & Hyatt, 2000). Chytridiomycosis, a disease caused by the fungal pathogen *Batrachochytrium dendrobatidis* (*Bd*), has caused epizootics (epidemics in wildlife) in amphibians throughout the globe on a scale unheard of in any other vertebrate group (Wake & Vredenburg, 2008). *Bd* infects the skin of amphibians and causes mortality by disrupting the skin electrolyte transport system (Voyles et al., 2012). However, interactions between *Bd* and other skin microbes, particularly bacteria, can inhibit *Bd* colonization and pathogenicity (Harris et al., 2009; Muletzwolz et al., 2017).

The community of microorganisms on amphibian skin includes bacteria, archaea, fungi and protozoans (Kueneman et al., 2013; Kueneman, Weiss, & McKenzie, 2017), but bacteria have been the focus of the majority of studies investigating microbial interactions with *Bd*. Hereafter, we refer to the community of bacteria as the skin microbiome. Just as some mutualistic skin microbes can inhibit *Bd* establishment in certain amphibian hosts (Harris et al., 2009; Muletz,

Myers, Domangue, Herrick, & Harris, 2012), *Bd* colonization, conversely, has the capacity to significantly disrupt the amphibian skin microbiome (Jani & Briggs, 2014). In this study, we use next-generation sequencing to closely examine the interaction between *Bd* infection and several metrics of microbiome diversity, including species richness, species evenness, phylogenetic diversity and variation between individual hosts. We then use traditional bacterial culturing techniques to characterize components of the amphibian skin microbial communities to assess functional differences.

This study focuses on the Sierra Nevada yellow-legged frog (*Rana sierrae*), which is one of the most threatened amphibian species in North America. *R. sierrae* live at mid to high elevations in the Sierra Nevada mountains and are extirpated from over 90% of their historical range (Vredenburg et al., 2007). Recent declines are due in large part to epizootic outbreaks of *Bd* followed by frog population collapse (Vredenburg, Knapp, Tunstall, & Briggs, 2010). Available evidence suggests that *Bd* arrived in the central Sierra Nevada in the 1970s (Ouellet, Mikaelian, Pauli, Rodrigue, & Green, 2005) (V. T. Vredenburg, unpublished data) and caused widespread *R. sierrae* population declines and extirpations. However, a few populations persisted through this epizootic event including our two study populations, located in the Desolation Wilderness of the Sierra Nevada mountains in California. These populations persist with *Bd* in an enzootic state, as evidenced by relatively stable numbers of adults and low infection intensities across life stages (see Results for additional information). Given the devastating impact of *Bd* in other species, and even in other populations of this same species, we assess whether the enzootic persistence of *Bd* with *R. sierrae* is modulated by the composition and structure of the skin microbial community (see also Jani & Briggs, 2014; Jani, Knapp, & Briggs, 2017).

To study *Bd* host–pathogen dynamics and the interaction of *Bd* with *R. sierrae*'s skin microbial communities, we conducted (a) a detailed temporal survey of *Bd* prevalence and infection intensity across all *Bd*-susceptible *R. sierrae* life stages, (b) a 16S rRNA community structure analysis of the skin microbiome of the same *R. sierrae* life stages and (c) laboratory culturing of field-derived skin bacterial isolates to identify bacteria that may influence frog-*Bd* dynamics and which may be potential candidates for bioaugmentation efforts against *Bd*. As chytridiomycosis continues to spread throughout the world, the interface of skin microbial communities with *Bd* in post-epizootic disease dynamics is a promising area to research to determine how species can persist despite infection with this destructive pathogen.

2 | MATERIALS AND METHODS

2.1 | Study site

Samples were collected from two populations in the Desolation Wilderness, CA ("Pyramid Valley" and "Rivendell Pond"). The habitats are comprised primarily of small ponds and lakes connected by streams in a landscape of granitic bedrock and sparse conifer trees. The two study populations are separated from one another by approximately 3 km and are not directly connected by water. The intervening landscape features a network of lakes and streams containing non-native fish, which makes the habitat unsuitable for *Rana sierrae* (Vredenburg, 2004). The elevation of water bodies occupied by these populations ranges from 2,450 to 2,542 m.

2.2 | *Batrachochytrium dendrobatidis* sampling and detection

To describe the disease dynamics in our study populations, we used standard *Bd* detection methods, as described in Vredenburg et al. (2010). Briefly, frogs were captured by hand and with dip nets along the shoreline of ponds and lakes, inlets and outlets, and nearby seasonal pools, and they were stroked 30 times on the ventral side using sterile Dacron swabs (five strokes on each side of the abdomen, thighs and plantar side of the hindlimbs). Tadpoles were swabbed with 30 strokes on the mouthparts. Swabs were air-dried and stored at 4°C until processing. DNA was extracted using PrepMan Ultra (Boyle, Boyle, Olsen, Morgan, & Hyatt, 2004), and *Bd* infection intensity was quantified using quantitative polymerase chain reaction (qPCR) (Hyatt et al., 2007) using an Applied Biosystems 7300 Real-Time PCR system. Samples were run singly, and the standards used were created using a strain of the highly virulent global pandemic lineage (*Bd*-GPL1) collected in 2009 in the southern Sierra Nevada (CJB7). Samples were considered positive for *Bd* if the output values were >0, and if amplification curves were sigmoidal and crossed the standard-generated threshold. Zoospore equivalent (ZE) scores were calculated by multiplying the raw qPCR output by 80 to account for the subsampling and dilution that occurs during DNA extraction (Briggs, Knapp, & Vredenburg, 2010; Vredenburg et al., 2010).

2.3 | Microbial community sample collection

Microbiome samples were collected from the skin of *R. sierrae* and from the ponds in which frogs were captured. Each frog or tadpole was handled with a new pair of gloves, and dip nets were rinsed thoroughly with pond water between captures. Prior to sample collection, each frog or tadpole was rinsed with 50 ml sterilized pond water to remove transient bacteria (Culp, Falkinham, & Belden, 2007; Lauer et al., 2007). The entire skin surface of the animal was swabbed with a sterile Dacron swab for 30 s. Swabs were transferred to sterile microcentrifuge tubes and stored on ice or dry ice for transportation to the laboratory and then stored at −80°C until processing.

To sample the microbial communities in pond water, we passed 250 ml of pond water through 0.22-μm Sterivex filters (Millipore). Water samples were collected for each frog population in the location where the highest density of adult frogs was captured. Water was collected approximately 1 m from the shoreline, and at least 10 mm below the surface and above the bottom of the pond. Filters were stored in sterile 60-ml tubes on ice or dry ice for transportation and then stored at −80°C until processing.

2.4 | Study design

We conducted this study in coordination with a related mark–recapture project intended to characterize the population size and recruitment dynamics of persistent *R. sierrae* populations in the Desolation Wilderness (R. A. Knapp, unpublished data). Thus, the criteria used for sample selection in the microbiome study were influenced by the study design of the mark–recapture project. In that project, we used 8 mm passive integrated transponder (PIT) tags inserted under the dorsal skin to permanently identify each study animal (Briggs et al., 2010). We targeted only adult frogs (≥40 mm) for inclusion in the mark–recapture effort to avoid potential negative effects of tagging smaller, juvenile frogs. Simultaneous with the tagging of each adult frog, we also collected a skin swab to quantify *Bd* infection intensity, as described above, and we collected additional *Bd* samples at each subsequent capture of that individual. We used a robust study design for the mark–recapture effort (Bailey, Kendall, Church, & Wilbur, 2004), surveying each frog population for three consecutive days (weather permitting) at one-month intervals throughout the summer active season (June–September).

A subset of adult frogs was selected for inclusion in the microbiome study with the aim of evaluating variability in the skin microbiome of individuals through time. Microbiome samples were collected, as described above, from all marked adult frogs in the first mark–recapture period (June 2013), and from all recaptured frogs in the second recapture period (July 2013). During August–September 2013 and June–September 2014, microbiome samples were collected only from frogs that had been captured in the June and July 2013 sampling periods. Samples included in our microbiome analysis were those from individuals with the highest number of repeated samples (ranging from 2 to 6 captures per animal). Microbiome samples were also collected from metamorphs, subadults and tadpoles, although we did not mark individuals of these life stages using PIT tags due to the previously mentioned constraints. Since each study population likely included thousands of metamorphs, subadults and tadpoles, we assume that no single animal was sampled more than once during the 2 years of microbiome sample collection. In our microbiome analysis, we included samples from metamorphs, subadults and tadpoles collected at the Rivendell Pond population only—since the number of samples from these life stages included in the microbiome analysis was limited, we used the single population to focus our analyses on the differences observed between life stages, rather than the effect of population on the microbiome of each life stage.

2.5 | Microbial community sample preparation

DNA was extracted from swabs and filters using the PowerSoil DNA Isolation Kit (MoBio Laboratories, Carlsbad, CA, USA), and sequencing libraries were prepared following the protocol "16S Metagenomic Sequencing Library Preparation" (Illumina, Inc., San Diego, CA, USA). Briefly, the hypervariable V3-V4 region of the bacterial 16S gene was PCR amplified using primers with overhang adaptors. PCR product for triplicate reactions was pooled and purified using solid phase reversible immobilization beads (Agencourt AMPure XT; Agencourt Bioscience Corporation, Beverly, MA, USA). All samples and negative controls were visualized using gel electrophoresis. Dual indices were attached to the purified amplicons using PCR, and the resulting PCR product was purified and visualized as described above. DNA concentrations were quantified using qPCR (KAPA Library Quantification Kit; KAPA Biosystems), and samples were diluted and pooled at equimolar concentrations. Sequencing was performed on an Illumina MiSeq using a MiSeq Reagent Kit v3 (600 cycles) (Illumina, Inc.).

2.6 | Bioinformatics

Base calling and demultiplexing were performed using MISEQ REPORTER (Illumina, Inc.). Unless otherwise specified, all bioinformatic analyses were conducted using QIIME (Caporaso, Kuczynski, et al., 2010). Paired-end reads were assembled, and the resulting sequences were quality filtered at a threshold of q20. Sequences were aligned using PYNAST (Caporaso, Bittinger, et al., 2010) and the GREENGENES core reference alignment (DeSantis et al., 2006). operational taxonomic units (OTUs) were determined using an open reference OTU picking strategy (Edgar, 2010) and a 97% sequence similarity threshold, and taxonomy was assigned using the GREENGENES Database version 13_8 (McDonald et al., 2012; Wang, Garrity, Tiedje, & Cole, 2007; Werner et al., 2012). An approximately maximum-likelihood phylogenetic tree was generated using FASTTREE 2.1.3 (Price, Dehal, & Arkin, 2010). Beta diversity was calculated using weighted and unweighted UniFrac distances (Lozupone & Knight, 2005) and visualized using EMPEROR (Vázquez-Baeza, Pirrung, Gonzalez, & Knight, 2013).

2.7 | Isolation and cryopreservation of bacterial morphotypes

To quantify the *Bd*-inhibitory properties of *R. sierrae*'s skin bacteria, we collected samples from the skin of 50 adult frogs (June 2013) and 10 juvenile frogs (July 2013), as described above. Swabs were transferred to sterile microcentrifuge tubes containing 1 ml of a weak salt solution (10 mM KH_2PO_4, 1 mM $MgCl_2$ and 0.2 mM $CaCl_2$) (Flechas et al., 2012) and stored on ice until processing. At the laboratory, each sample was diluted by serial, 10-fold dilutions to a concentration of 10^{-5}. 100 μL of the 10^{-3}, 10^{-4} and 10^{-5} dilutions was transferred to Petri dishes containing R2A, a low nutrient growth medium (Reasoner & Geldreich, 1985). After approximately 1 week of incubation at 21°C, unique morphotypes of bacteria were identified based on differences in colour, texture, growth form and other morphological features. Forty-five morphotypes were identified, streaked on 1% tryptone agar plates and incubated at 21°C. Once pure cultures of each morphotype were obtained, isolates were cryopreserved in nutritive broth with 30% glycerol at −80°C.

2.8 | *Bd* inhibition assay

We tested each isolate for activity inhibiting or facilitating the growth of *Bd* using a cell-free supernatant (CFS) inhibition assay (Bell, Alford, Garland, Padilla, & Thomas, 2013). In this technique, *Bd* is grown in culture with the metabolites isolated from each bacterial isolate, and inhibition or facilitation is quantified by measuring the change in optical density over a period of 6 days. In an adapted version of a previously published protocol (Bell et al., 2013), 50 µl zoospore suspension containing approximately 230,000 zoospores of cultured *Bd-GPL (strain id#CJB57*, collected during a *R. sierrae* mass die-off event in the southern Sierra Nevada in 2011) was challenged against the various bacterial isolate supernatants in replicates of 5 (CFS was collected after culturing approximately 10 µl of each isolate in 2 ml of 1% tryptone broth at 26 C for 3 days). The optical density at 490 nm in each well was measured every 24 hr using a SpectraMax 190 Microplate Reader and the SOFTMAX PRO software. The total change in optical density after 7 days was used as a proxy for *Bd* growth, which we defined as the percentage increase in optical density over the course of 6 days, averaged over the five replicates for each isolate.

2.9 | CFS isolate sequencing and identification

DNA was extracted from liquid cultures using CHELEX, and the hypervariable V3-V4 regions of the bacterial 16S gene were amplified using PCR (F: 5′- CCTACGGGNGGCWGCAG; R: 5′-GACTACHVGGGTATCTAATCC) (Klindworth et al., 2013). Each 25 µl reaction consisted of 12 µl 5 PRIME HotMasterMix (5 PRIME, Inc., Gaithersburg, MD, USA), 10 µl PCR water, 1 µl forward and reverse primers (10 µM), and 1 µl template. PCR conditions were 95°C for 120 s, followed by 35 cycles of 95°C for 30 s, 56°C for 30 s and 72°C for 60 s, and a final extension of 72°C for 300 s. All samples and negative controls were visualized using gel electrophoresis. PCR product was purified using ExoSAP-IT (Affymetrix, Santa Clara, CA, USA). Cycle sequencing was performed using 12 µl reactions, consisting of 0.5 µl Big Dye Terminator v3.1 (Life Technologies, Grand Island, NY, USA), 2.2 µl 5× buffer, 1 µl sequencing primer (same as amplicon primers), 5.3 µl PCR water and 3 µl template. Cycle sequencing conditions were 94°C for 90 s, followed by 25 cycles of 94°C for 20 s, 58°C for 30 s and 72°C for 240 s. Purification and precipitation were performed using 125 mM EDTA and 0.11 M sodium acetate in ethanol. DNA was air-dried for 5 min, resuspended in Hi-Di formamide (Life Technologies) and sequenced in both directions using an ABI 3100 Genetic Analyzer (Life Technologies).

Base calling was performed using SEQUENCING ANALYSIS 5.1 (Applied Biosystems), and sequences were assembled, trimmed and quality-controlled using SEQUENCHER 4.8 (Gene Codes Corporation). Taxonomy was assigned using QIIME and the GREENGENES Database version 13_8 (McDonald et al., 2012; Wang et al., 2007; Werner et al., 2012), as described above. Sequence similarity between the CFS isolates and the corresponding OTUs from the metabarcoding data set was determined using BLASTN (Altschul, Gish, Miller, Myers, & Lipman, 1990).

2.10 | Statistical analysis

The relationship between *Bd* infection intensity (log ZE) and frog snout-vent length (SVL) was examined using linear regression. We tested for differences in mean infection intensity between frog size classes using ANOVA with post hoc Tukey honest significant difference (HSD) tests. Similarly, we tested for differences in OTUs per sample between sample types using ANOVA with post hoc Tukey HSD tests. To test for differences in infection intensity between populations, we used a generalized additive model, where infection intensity was the response variable, and SVL and population were predictor variables.

Exploratory data analysis revealed that the skin microbiome of post-metamorphic frogs with infection intensities exceeding 1,000 ZE differed markedly from frogs with lower infection levels, and we found that this trend was best characterized by a categorical, rather than a linear, relationship. Thus, for all following microbiome analyses, we classified frogs as having either a "High ZE" (>1,000 ZE) or a "Low ZE" (<1,000 ZE) infection intensity. It should be noted, however, *R. sierrae* typically suffer mortality from chytridiomycosis at a higher threshold (>10,000 ZE) (Vredenburg et al., 2010), so frogs in the "High ZE" group do not necessarily host lethal *Bd* infection loads.

In addition, all the post-metamorphic frogs in our data set with infection intensities above 1,000 ZE were recently metamorphosed juveniles, so it is possible that the differences we observed in the microbiome of "High ZE" and "Low ZE" infected frogs were actually the result of age, rather than infection intensity. In order to determine whether age or infection intensity contributed more significantly to the observed microbiome differences, we used the biota–environmental matching procedure (BIO-ENV) (Clarke & Ainsworth, 1993) as implemented in QIIME. In the BIO-ENV analysis, we used weighted UniFrac distances as the community dissimilarity matrix, and we used infection category, SVL and a combination of the two as variables. Throughout this paper, we primarily present results from the "High ZE"/"Low ZE" interpretation, and we consider alternative possible interpretations of our results in the discussion section.

We used several tests to compare bacterial composition between frog groups. We compared bacterial beta diversity between groups using a permutation-based ANOVA (PERMANOVA). To compare species composition between groups, we used unweighted UniFrac distances, and to compare community structure, we used weighted UniFrac distances (Lozupone & Knight, 2005). To compare variability in species composition and community structure between groups, we used a parametric *t* test with Bonferroni correction. We quantified species richness using "observed OTUs," and we quantified species evenness, defined as (Shannon entropy)/$\log_2$ (number of observed OTUs). We compared alpha diversity between groups using nonparametric two-sample *t* tests with 999 Monte Carlo permutations.

To compare the relative abundances of bacterial taxa of interest, we used ANOVA or a two-sample *t* test. 95% Bayesian credibility intervals for the prevalence of bacterial taxa were calculated using the "prevalence" package in R, and we determined whether prevalences differed significantly between groups using Fisher's exact tests.

In the CFS *Bd* inhibition assay, inhibitory strength for each isolate was calculated as [1 − (Isolate *Bd* growth/Positive control *Bd* growth). Significance of *Bd* inhibition was calculated by comparing the *Bd* growth of each isolate with the *Bd* growth of the positive control and conducting a two-sample *t* test. The significance of differences in relative abundances of each bacterial OTU between the "High ZE" and "Low ZE" groups was also calculated using a *t* test.

3 | RESULTS

3.1 | Patterns of *Bd* infection in the study populations

During the 2012–2014 study period, we collected a total of 1,577 *Bd* swabs (Pyramid Valley population: $n = 787$; Rivendell Pond population: $n = 790$) from 877 individual *Rana sierrae* (Pyramid: 434; Rivendell: 443) during the summer active season (June–September). The majority, 1,463, were collected from adult frogs (>40 mm SVL) (Pyramid: $n = 725$; Rivendell: $n = 738$), 18 from subadults (32 mm < SVL < 40 mm) (Pyramid: $n = 15$; Rivendell: $n = 3$), 54 from metamorphs (<32 mm SVL) (Pyramid: $n = 25$; Rivendell: $n = 29$) and 42 from tadpoles (Pyramid: $n = 22$; Rivendell: $n = 20$). Among tadpoles, which typically develop for 2 years before undergoing metamorphosis, and which harbour *Bd* infection only in their keratinized mouthparts, there was a strong positive correlation between infection intensity and Gosner stage (Figure 1; Pyramid: $p = 0.009$, $R^2 = 0.29$; Rivendell: $p < 0.0001$, $R^2 = 0.82$; linear regression). Among post-metamorphic frogs, infection intensities decreased steeply with increasing frog size up to approximately 40 mm SVL and then remained relatively constant in frogs up to 75 mm SVL. Of the three size classes, metamorphs showed the highest infection levels (Pyramid: $p < 0.0001$, $F = 52.82$, $df = 3$; Rivendell: $p < 0.0001$, $F = 52.65$, $df = 3$; ANOVA with Tukey HSD post hoc tests), and in this size class, there was a strong negative relationship between infection intensity and SVL (Pyramid: $p = 0.004$; $R^2 = 0.39$; Rivendell: $p = 0.0003$, $R^2 = 0.39$; linear regression). Subadults exhibited high variability in infection intensity and no significant linear pattern between infection intensity and SVL (Pyramid: $p = 0.453$, $R^2 = 0.044$; Rivendell: $p = 0.499$, $R^2 = 0.501$; linear regression); adults similarly exhibited no significant relationship between SVL and infection intensity (Pyramid: $p = 0.514$, $R^2 = 0.001$; Rivendell: $p = 0.078$, $R^2 = 0.004$; linear regression). There was a statistically significant difference in infection intensities between our two study populations (GAMM; $p < 0.0001$, $F = 55.1$, $df = 1$; Supporting Information Figure S1) although the difference was small relative to infection thresholds known to seriously impact host health (e.g., Pyramid adult mean = 0.99 log ZE [±0.95]; Rivendell adult mean = 0.64 log ZE [±0.80]; compared with mortality threshold at 4 log ZE).

3.2 | Microbial communities in frog and environmental samples

After assembly and quality filtering, a total of 4,704,549 microbial DNA sequences were included in the microbiome analysis, representing 24,118 OTUs. After rarefying at an even sampling depth of 15,030 sequences per sample (the lowest number of sequences obtained from any individual sample), 1,923,840 sequences remained, representing 329 orders of bacteria and 10 orders of archaea. An average of 683 OTUs was detected on adult frogs; 444 OTUs/sample on metamorphs and subadults; 547 OTUs/sample on tadpoles; and 1,708 OTUs/sample from water samples. The number of OTUs/sample were not significantly different between frog size classes (adults vs. tadpoles: $p = 0.72$; adult vs. metamorphs and subadults: $p = 0.17$; tadpoles vs. metamorphs and subadults: $p = 0.91$; ANOVA

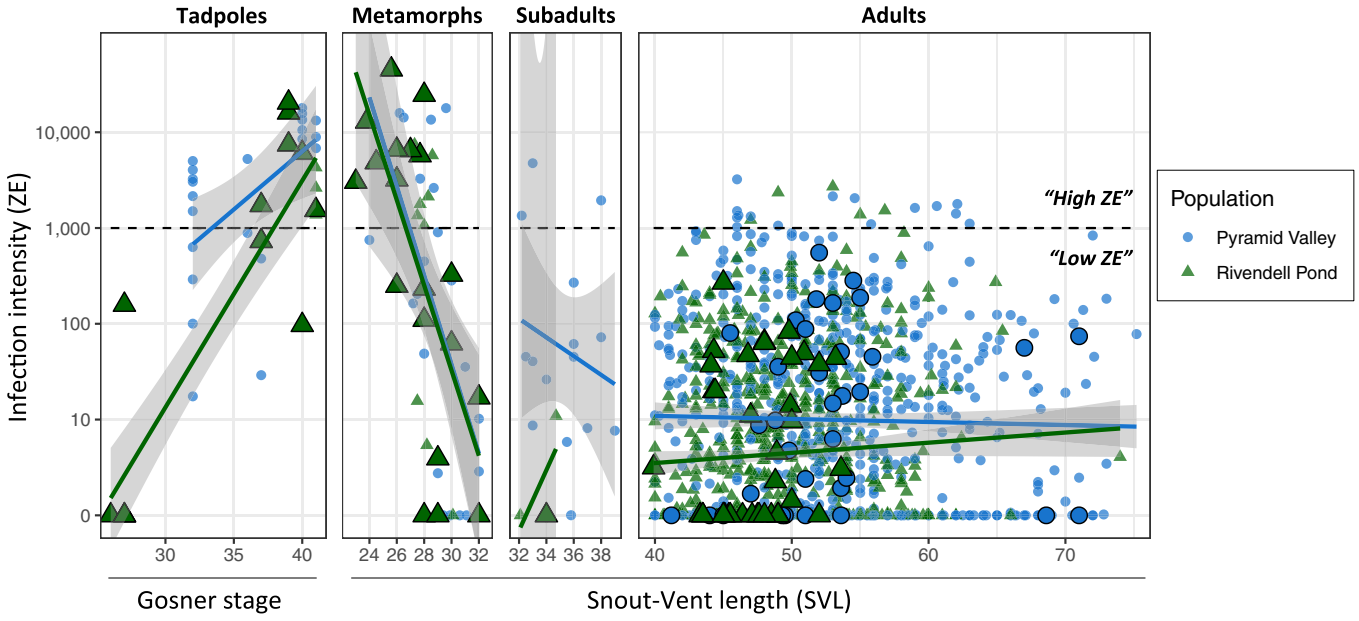

FIGURE 1 *Bd* infection intensities of tadpoles and frogs in the study area, described using linear regression. Shaded regions represent 95% confidence intervals, and large outlined points indicate samples that were included in the microbiome analysis

with Tukey HSD post hoc tests), but water samples had a significantly higher number of OTUs/sample than all other sample types ($p < 0.0001$, ANOVA with Tukey HSD post hoc tests). Among adults, there were significant differences in microbial communities between the two study populations, both in terms of species composition ($p = 0.001$, pseudo-$F = 1.843$, $df = 1$, PERMANOVA) and community structure ($p = 0.047$, pseudo-$F = 2.016$, $df = 1$, PERMANOVA). Juveniles and tadpoles were only sampled at the Rivendell Pond population, so differences in population could not be assessed. Water samples were significantly different between the two populations in terms of community structure ($p = 0.002$, pseudo-$F = 6.562$, $df = 1$, PERMANOVA) but not species composition ($p = 0.237$, pseudo-$F = 1.128$, $df = 1$, PERMANOVA).

3.3 | *Bd* and microbiome diversity

Among post-metamorphic frogs, we detected few significant differences between the microbial communities of *Bd*-negative individuals (Pyramid: $n = 10$; Rivendell: $n = 23$) and those with low to moderate infection levels (<1,000 ZE; Pyramid: $n = 25$; Rivendell: $n = 30$). In the Rivendell population, these groups differed significantly in terms of species composition ($p = 0.034$, pseudo-$F = 1.338$, $df = 1$, PERMANOVA); however, in the Pyramid Valley population, there was no significant difference (Pyramid: $p = 0.98$, pseudo-$F = 0.802$, $df = 1$). In both populations, there were no significant differences between the microbial communities of *Bd*-negative frogs and those with low to moderate infection levels in terms of community structure (Pyramid: $p = 0.464$, pseudo-$F = 0.899$, $df = 1$; Rivendell: $p = 0.068$, pseudo-$F = 1.829$; PERMANOVA), species richness (Pyramid: $p = 0.403$, $t = -0.873$, $df = 10.4$; Rivendell: $p = 0.240$, $t = 1.190$, $df = 50.5$; t test) or species evenness (Pyramid: $p = 0.448$, $t = -0.779$, $df = 15.1$; Rivendell: $p = 0.247$, $t = -1.173$, $df = 42.3$; t test).

However, microbial communities of post-metamorphic frogs that had infection intensities above 1,000 ZE and below 1,000 ZE were significantly different in the Rivendell population (no post-metamorphic frogs in the Pyramid population had infection levels that exceeded 1,000 ZE, so we excluded them from these comparisons). Principal coordinates analysis using weighted and unweighted UniFrac distances (Lozupone & Knight, 2005) revealed that the skin microbiome of "High ZE" infected frogs (> 1,000 ZE; Rivendell: $n = 9$) was a greatly restricted subset of the more diverse array of microbial communities found in frogs with lower infection levels (<1,000 ZE; Rivendell: $n = 53$; Figure 2). This "High ZE" subset, which is significantly distinct from the "Low ZE" group in terms of both species composition (Rivendell: $p = 0.001$, pseudo-$F = 2.372$, $df = 1$, PERMANOVA) and community structure (Rivendell: $p = 0.002$, pseudo-$F = 5.236$, $df = 1$, PERMANOVA), is characterized by dramatically reduced alpha and beta diversity (Figure 3). Species richness was significantly reduced in highly infected frogs (Rivendell: $p < 0.0001$, $t = -7.005$, $df = 58.3$, t test), and species evenness was also significantly reduced (Rivendell: $p < 0.0001$, $t = -7.200$, $df = 18.3$, t test).

Beta diversity was also significantly reduced among post-metamorphic frogs classified as "Highly" infected. Species composition was much less variable among highly infected frogs than among frogs with lower infection levels, as measured by unweighted UniFrac distances (within "High ZE" vs. within "Low ZE", Rivendell: $p < 0.0001$, $t = -9.012$, $df = 40.0$, t test with Bonferroni correction). Similarly, there was significantly less variation in community structure among highly infected frogs than among other frogs, as measured by weighted UniFrac distances (within "High ZE" vs. within "Low ZE", Rivendell: $p < 0.0001$, $t = -45.033$, $df = 85.8$, t test with Bonferroni correction). Thus, *R. sierrae* with high *Bd* infection intensities host a homogenous skin microbiome with a relatively small number of species and low phylogenetic diversity, and with very little variation in species composition and community structure between individuals.

3.4 | *Bd* and taxonomic diversity

The skin microbiome of post-metamorphic frogs in the "Low ZE" and "High ZE" infection groups also differed significantly in the

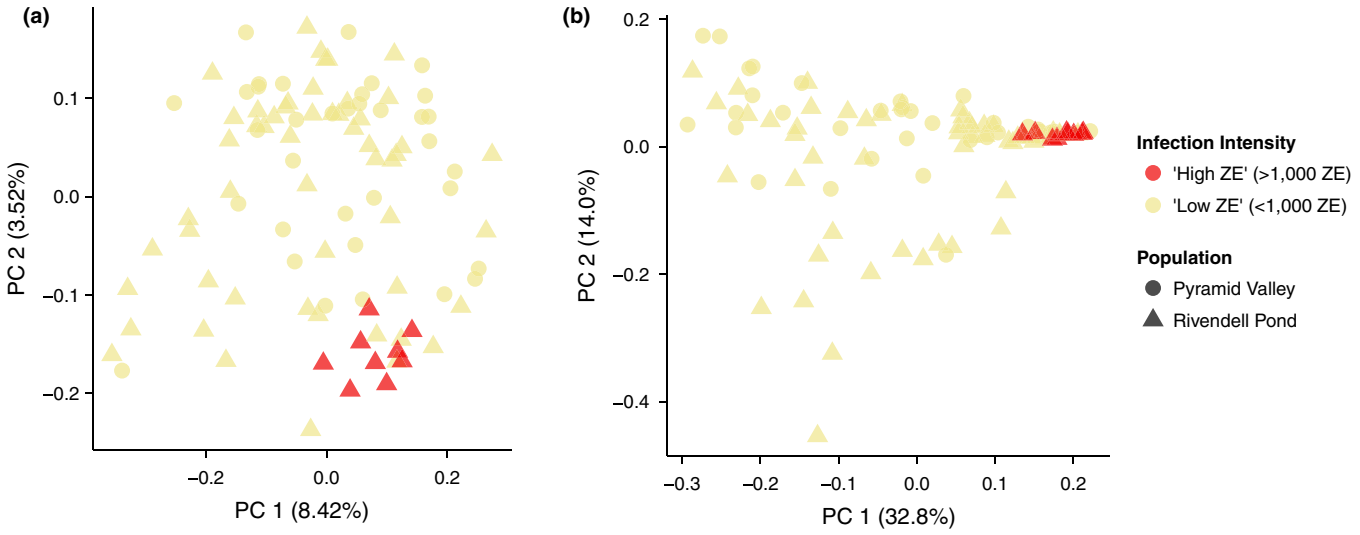

FIGURE 2 Principle coordinates analysis (PCoA) plots, using unweighted UniFrac distances (a) and weighted UniFrac distances (b)

relative abundance of bacteria in the order Burkholderiales. On average, 90% of the DNA sequences obtained from post-metamorphic frogs in the "High ZE" group were derived from this single order, compared to an average of 52% for frogs in the "Low ZE" group (Rivendell: $p < 0.0001$, $t = 9.557$, $df = 51.2$, t test; Figure 3). In addition, there was much less variation in the relative abundance of Burkholderiales in the highly infected group: Abundances ranged from 78.0% to 96.4% in the highly infected group, while abundances ranged from 7.2% to 95.0% among frogs with lower infections. The vast majority of the Burkholderiales sequences are derived from previously undescribed genera in the family Comamonadaceae (83.6% of total sequences for highly infected frogs; 48.5% for other frogs; Rivendell: $p < 0.0001$, $t = 7.294$, $df = 28.9$, t test). Other families we detected in order Burkholderiales included (in decreasing order of relative abundance) the following: Oxalobacteraceae, Alcaligenaceae and Burkholderiaceae. *Janthinobacterium lividum*, the species most widely used in probiotic treatments to date (Becker et al., 2011; Harris et al., 2009; Kueneman, Woodhams, Harris, et al., 2016), a member of the order Burkholderiales and family Oxalobacteraceae, was detected in 33% (CI: 10.4%–65.2%, Rivendell) of highly infected frogs and 58.5% (CI: 45.1%–71.0%, Rivendell) of frogs with lower infection levels, but this difference was not statistically significant (Rivendell: $p = 0.87$, Fisher's exact test). The relative abundance of *J. lividum* was lower on highly infected frogs, but this difference was not statistically significant, and mean relative abundances were quite low in all samples (Rivendell "High ZE": 0.0002% total sequences; Rivendell "Low ZE": 0.001%; $p = 0.08$, $t = -1.794$, $df = 32.0$, t test).

3.5 | *Bd* and the microbiome of tadpoles

The microbiome of tadpoles did not reflect the patterns observed among post-metamorphic frogs described above. We did not detect significant differences between "High ZE" tadpoles ($n = 8$) and "Low ZE" tadpoles ($n = 8$) in terms of species composition, community structure, species richness, species evenness, beta diversity or the abundance of Burkholderiales (all $p > 0.05$; see SI Results for complete results). The order Burkholderiales, which dominated the microbiome of post-metamorphic frogs, accounted for only 16.3% of DNA sequences detected among tadpoles; instead, the tadpole microbiome was dominated by the family Chitinophagaceae (order: Saprospirales), which accounted for an average of 47.7% of DNA sequences detected among tadpoles. The relative abundance of Chitinophagaceae also did not differ significantly between "High ZE" tadpoles (48.7%) and "Low ZE" tadpoles (47.0%) ($p = 0.91$, $t = 0.121$, $df = 10.17$, t test).

3.6 | Host attributes correlated with microbiome changes

Notably, all the post-metamorphic individuals in our data set with a "High ZE" infection level were recently metamorphosed frogs (Figure 1). To determine whether infection intensity or age (as represented by SVL) was more strongly associated with the microbiome changes we observed, we employed the biota–environmental matching procedure (BIO-ENV), as implemented in QIIME (Table 1). The BIO-ENV analysis revealed that the variable most correlated with differences in community structure was *Bd* infection category ($\rho = -0.119$), followed closely by *Bd* infection category +SVL ($\rho = -0.108$); SVL alone had a correlation coefficient closer to 0 ($\rho = -0.037$). Thus, we concluded that infection intensity was more strongly correlated with the observed microbiome changes, but we explore alternative interpretations in the Discussion.

3.7 | CFS Isolate Identification and *Bd* Inhibition

A total of 43 bacterial isolates were cultured from field-collected swabs; however, sequencing analysis and subsequent taxonomy

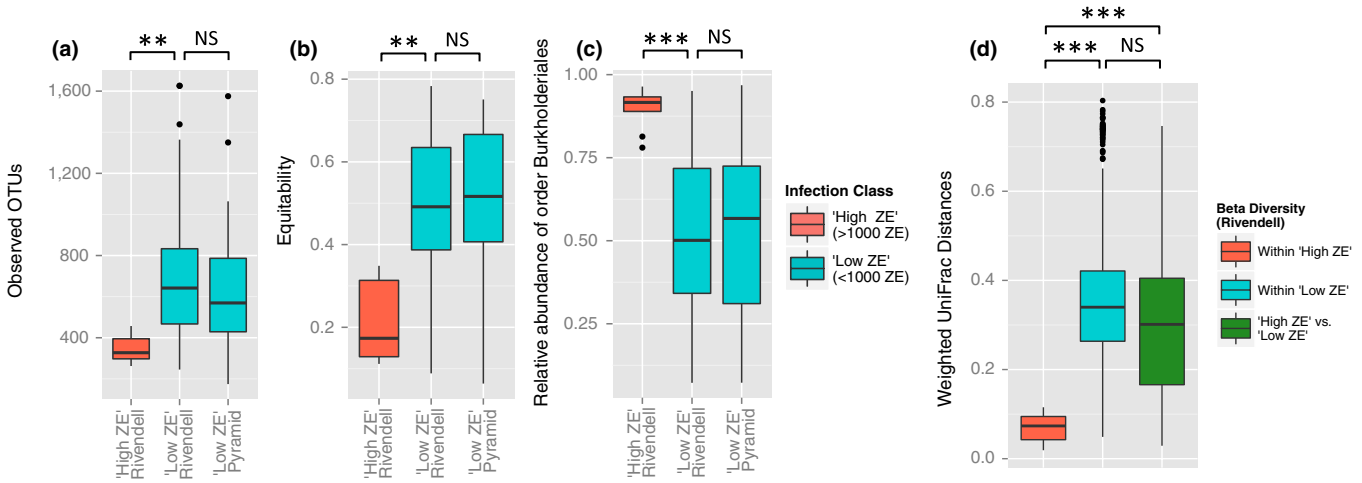

FIGURE 3 Microbial community differences between "High ZE" and "Low ZE" groups. Species richness (a), species evenness (b), relative abundance of the order Burkholderiales (c) and variability in community structure (d). Asterisks represent statistical significance (*<0.05; **<0.005; ***<0.0005; NS = not significant), using nonparametric t tests with 999 Monte Carlo permutations (a) and parametric t test with Bonferroni correction (b)

TABLE 1 Correlations of frog characteristics and microbiome community structure (weighted UniFrac distances), generated using BIO-ENV

Variables	Spearman's rank correlation coefficient (ρ)	$\Delta\ \lvert\rho\rvert$
Bd infection category	−0.119	0.000
Bd infection category +SVL	−0.108	−0.011
SVL	−0.037	−0.082

assignment revealed that these isolates represented just nine unique OTUs, so the results from replicates of each OTU were averaged (results for each individual isolate, along with sequence similarity data, are presented in Supporting Information Table S1). Sequence similarity between each isolate and the corresponding OTUs in the metabarcoding data set was ≥99% in all cases. The isolates represented five orders of bacteria in three phyla: Bacteroidetes, Firmicutes and Proteobacteria. The metabolites derived from the bacterial isolates had a range of effects on the growth of *Bd*, from moderate inhibition (57% reduction in growth compared to positive control) to near complete inhibition (97% reduction in growth) (Table 2). All isolates led to a statistically significant reduction in *Bd* growth, and no isolates facilitated the growth of *Bd*. An unclassified species of *Pseudomonas* had the strongest inhibitory effect, with 97% inhibition, while an unidentified species in family Enterobacteriaceae had the mildest inhibitory effect, with 57% inhibition observed. A strain of *J. lividum* was included in the CFS inhibition trials, and it demonstrated strong inhibition of *Bd* growth (75% inhibition compared to the positive control, $p = 0.005$, $t = -4.719$, $df = 4.9$, t test). One other unclassified genus in family Oxalobacteraceae (order: Burkholderiales) was included in the trials and demonstrated a similarly strong inhibitory effect (72% inhibition, $p = 0.008$, $t = -4.741$, $df = 4.2$, t test), but no members of family Comamonadaceae (the most common family in the skin microbiome) were cultured. The mean relative abundance of two isolates (*Flavobacterium succinicans*, $p = 0.001$, $t = -3.4338$, $df = 52$; and a member of an unclassified genus in family Enterobacteriaceae, $p = 0.023$, $t = -2.3448$, $df = 53.151$) was significantly greater in the "Low ZE" group (Rivendell only) than in the "High ZE" group (Rivendell only), and these isolates all strongly inhibited the growth of *Bd* (the relative abundance of a third isolate, *J. lividum*, had a nearly significant difference between the "High ZE" and "Low ZE" groups [$p = 0.055$, $t = -1.9587$, $df = 54.938$] and also strongly inhibited the growth of *Bd*). In contrast, the mean relative abundance of the other six bacterial isolates did not differ significantly between the "High ZE" and "Low ZE" groups (Rivendell only; Table 2).

4 | DISCUSSION

4.1 | *Bd* and skin microbiome diversity

In this study, we examined the effects of *Bd* infection on the skin microbiome of two post-decline, enzootic populations of *Rana sierrae*, a species that has experienced major declines due to *Bd* epizootics. We found that the skin microbiome of *Bd*-negative, post-metamorphic frogs did not differ significantly from frogs with low to moderate infection levels (<1,000 ZE), except species composition in the Rivendell population. However, the skin microbiome of more highly infected, post-metamorphic frogs (>1,000 ZE) was characterized by dramatic reductions in species richness, species evenness, phylogenetic diversity and variability in species composition and community structure between individuals. Two other studies investigating the same system (Jani & Briggs, 2014; Jani et al., 2017) found no significant correlation between an individual's *Bd* infection level and microbial community diversity; however, a recent study of montane frogs in the Pyrenees similarly found that frogs in epizootic populations hosted bacterial communities with lower alpha diversity than those from enzootic populations (Bates et al., 2018). We found that bacteria in the order Burkholderiales dominated the skin microbiome of highly infected frogs, accounting for 90% of bacterial DNA sequences derived from these animals, compared to just 54% of sequences among animals with lower infection levels. Bates et al. (2018) also found that the relative abundance of an unclassified family in order Burkholderiales was significantly impacted by the disease dynamics of the study population, but they detected significantly higher relative abundances in enzootic populations. The skin microbiome of tadpoles did not differ significantly between "High ZE" and "Low ZE" groups by any of these metrics. The relative abundance of two bacterial species which significantly reduced the growth of *Bd* in vitro was also reduced among highly infected frogs, suggesting that highly infected individuals may benefit less from the antifungal effects of these species.

4.2 | Host attributes correlated with microbiome changes

While infection intensity appears to be the factor most strongly correlated with the bacterial community changes we observed in our study populations, it is possible that other variables contributed to these patterns as well. The infection patterns across life stages in our enzootic study populations, as illustrated in Figure 1, reveal that the majority of "High ZE" animals (>1,000 ZE) in these populations are late-stage tadpoles and metamorphs. Indeed, all of the "High ZE" frogs included in the *Bd*-microbiome analysis were metamorphs with SVL <30 mm. Thus, an alternative interpretation of our results is that the microbiome differences we observed are actually due to the host's age and only incidentally related to infection intensity. Under this interpretation, the skin of frogs undergoing metamorphosis is initially colonized by a relatively simple community of microbes, but this community grows in complexity as the frogs reach adulthood.

We view both these interpretations as logical and parsimonious, and a priority in our analysis was determining which factor (infection intensity or age) was more strongly correlated with the microbiome differences we observed. Our statistical analyses suggest that infection intensity, and not age, was the most important factor driving microbiome diversity. For this reason, in this paper we primarily presented results comparing the microbiome of frogs

TABLE 2 Inhibitory strength (per cent *Bd* inhibition compared to the positive control), taxonomic classification, relative abundance and prevalence of isolates included in *Bd* inhibition trials

Family	Species identified	Number of isolates	Inhibitory strength [Mean (*SD*)]	Significance (*t* test)	"High ZE" mean relative abundance (%)	"Low ZE" mean relative abundance (%)	Significance (*t* test)	"High ZE" prevalence (%)	"Low ZE" prevalence (%)
Bacteroidetes (phylum)									
Flavobacteriaceae	*Flavobacterium succinicans*	2	86.2% (12.7%)	0.003**	0.000	0.034	0.001**	0	43
Firmicutes (phylum)									
Bacillaceae	*Bacillus flexus*	4	83.5% (12.3%)	0.004**	0.000	0.006	0.321	0	2
Proteobacteria (phylum)									
Enterobacteriaceae	Unclassified	10	78.7% (25.6%)	0.005**	0.033	0.086	0.023*	67	75
	Unclassified	3	56.5% (40.4%)	0.014*	0.180	0.428	0.163	100	91
Oxalobacteraceae	*Janthinobacterium lividum*	2	74.6% (15.9%)	0.005**	0.008	0.074	0.055†	33	58
	Unclassified	2	71.8% (7.3%)	0.008**	6.055	2.534	0.152	100	100
Pseudomonadaceae	*Pseudomonas fragi*	1	64.6% (4.6%)	0.012*	0.083	0.077	0.920	56	77
	Pseudomonas sp.	1	96.8% (3.6%)	0.003**	0.007	0.008	0.735	44	53
	Pseudomonas sp.	18	68.8% (28.2%)	0.009**	2.825	3.678	0.574	100	100

Note. Relative abundance and prevalence data include frogs from the Rivendell population only.
Asterisks represent statistical significance
†(<0.10; *<0.05; **<0.005).

with "High ZE" versus "Low ZE". Nonetheless, the metamorphs' concurrent development of a mature microbiome simultaneously with their infection and recovery from high *Bd* infection levels presents a fascinating case study in which to investigate the interaction between these two influences, and we suggest that the microbiome of *R. sierrae* metamorphs represents a rich ground for future research.

4.3 | Causation in the *Bd*-microbiome interaction

The underlying mechanism responsible for driving the microbiome patterns we describe here is impossible to determine, given the observational nature of this study. It is possible that infection with *Bd* disrupts the *R. sierrae* skin microbiome and that the low microbiome diversity observed among "High ZE" frogs is a direct result of *Bd* invasion. Conversely, it is possible that certain bacterial assemblages facilitate the invasion of *Bd*—that is, frogs in the "High ZE" group could have developed high infection levels because of the low diversity of their skin microbiome. In one of the only other studies of the *R. sierrae* skin microbiome published to date, Jani and Briggs (2014) used an experiment to demonstrate that *Bd* infection disrupts the *R. sierrae* skin microbiome and not the reverse. Many of our results are in concordance with Jani and Briggs (2014) (e.g., both studies found an increase in the relative abundance of bacteria in the order Burkholderiales and decreases in the relative abundance of most other taxa); therefore, we find it likely that *Bd* infection is the causative agent underlying the patterns we observed as well. However, further experimental studies are needed to fully delineate the effects of *Bd* on the microbiome versus the effects of the microbiome on *Bd*.

4.4 | No effect of *Bd* infection in the skin microbiome of tadpoles

We did not detect significant correlations between *Bd* infection and any of the metrics of change in the skin microbiome of tadpoles that we examined. This is not surprising, given that *Bd* infects only the keratinized mouthparts of *R. sierrae* tadpoles, whereas post-metamorphic frogs can develop high levels of infection throughout the entire surface of the skin (when collecting microbiome samples from tadpoles, we swabbed the entire surface of the tadpole, including the mouthparts). It is possible that *Bd* locally impacts the resident microbial communities of the mouthparts of tadpoles; however, further research will be needed to examine this possibility.

4.5 | Microbiome diversity: an indirect impact of *Bd* infection on host health

The direct pathogenic impacts that *Bd* causes in susceptible amphibian species have been well documented: *Bd* impairs osmoregulation, respiration and other physiological functions, leading to cardiac arrest and death (Voyles et al., 2009). The clinical symptoms and mortality associated with chytridiomycosis are usually observed in *R. sierrae* among post-metamorphic frogs, and only once an individual's infection level surpasses a threshold of approximately 10,000 ZE (Kinney, Heemeyer, Pessier, Lannoo, & Samples, 2011; Vredenburg et al., 2010). In our study, we found that *Bd* infection level was strongly associated with the degree of community diversity and variability between individuals in the skin microbiome, even among animals with infection levels below this 10,000 ZE threshold. This is significant because it suggests that individuals and enzootic populations persisting with sublethal infection levels may still be experiencing negative consequences due to the presence of *Bd*.

The shifts in microbial community structure we observed in highly infected frogs could lead to negative effects on host health in a variety of ways. In humans and mice, changes in microbial community membership (e.g., unweighted UniFrac) and structure (e.g., weighted UniFrac) have been shown to affect the ecological functions performed by the skin-associated microbiome and are associated with conditions such as obesity and diabetes (Tilg & Kaser, 2011; Turnbaugh et al., 2009). Changes in the microbiome of *R. sierrae* could similarly lead to chronic disease among highly infected frogs. Changes in microbiome community structure may also enhance or disrupt any defences that resident microbes provide to the host against infection with *Bd* (e.g., via the production of antifungal metabolites), thus affecting host health indirectly (Woodhams et al., 2014). In our study, several bacterial isolates that strongly inhibited the growth of *Bd* in vitro were significantly less abundant on frogs in the "High ZE" group than those in the "Low ZE" group, suggesting that the antifungal metabolites produced by these bacterial taxa may also be reduced or absent on "High ZE" frogs. The high degree of sequence similarity (≥99%) between the cultured bacterial isolates and the corresponding OTUs in the metabarcoding data set supports such functional comparisons; however, the limited number of isolates included in our inhibition trials (nine cultured isolates, none from family Comamonadaceae, compared with 24,118 OTUs detected in the metabarcoding study, in which Comamonadaceae was the most abundant family) clearly limits the scope of the inferences that can be made regarding changes in bacterial community function in highly infected frogs. Further studies incorporating both culture-independent bacterial community profiling and more holistic measures of bacterial community function will be needed to come to more definitive conclusions regarding the effects of *Bd* infection on the synthesis of defensive metabolites and other microbial community functions.

The reduction in alpha diversity (species richness, species evenness and taxonomic diversity) that we observed in highly infected frogs could have a similarly negative impact on host health. Evidence from other systems suggests that microbial community diversity is often correlated with the breadth of ecological functions performed by a community. In the human microbiome, taxonomic diversity is positively correlated with diversity of metabolic functions and pathways across a variety of locations on the body, including the skin, gut, oral cavity and vagina (Huttenhower et al., 2012). Similarly, human

patients with ileal Crohn's disease exhibit significantly reduced alpha diversity and correspondingly marked shifts in metabolic profiles (Balzola, Bernstein, & Ho, 2011). We hypothesize that the reduction in alpha diversity observed in highly infected frogs is likely to restrict the range of ecological functions performed by a more complex microbiome, and we suggest that further research should investigate this relationship.

4.6 | Microbiome diversity and host immunity

Evidence from other systems also suggests that the reduction in alpha and beta diversity that we observed in highly infected frogs could impair *R. sierrae*'s extended immune function. Decreased alpha diversity could facilitate pathogen invasion, by *Bd* or other infectious diseases, by reducing the efficiency of a community's utilization of limiting resources via niche specialization or by decreasing microheterogeneity (Costello, Stagaman, Dethlefsen, Bohannan, & Relman, 2012; Levine & Antonio, 1999; Lozupone, Stombaugh, Gordon, Jansson, & Knight, 2012). Decreased alpha diversity has also been shown to compromise community resilience by reducing or eliminating functional redundancy (Elmqvist et al., 2003), or by reducing the likelihood that a microbial community member is present that can combat an invasive pathogen through the synthesis of metabolites. This hypothesis is supported by the reduced abundance of strongly inhibitory bacteria among highly infected frogs we observed in this study. Decreased beta diversity may impair the resilience of host populations in the face of pathogen invasion by decreasing the likelihood that some individuals host a microbiome that can resist invasion. While these possibilities are intriguing, experimental manipulation of microbiome diversity in a controlled setting will be needed to definitively characterize the relationship between microbiome diversity and host/population invasibility.

4.7 | *Bd* infection intensity and age

In this study, we documented a strong negative correlation between size (SVL) and *Bd* infection intensity among metamorphs and subadults (SVL < 40 mm). The smallest post-metamorphic frogs nearly all had infection intensities >1,000 ZE, but infection intensity decreased by two orders of magnitude as SVL increased to 40 mm, and then remained relatively constant at just under 10 ZE among adults frogs. This correlation is likely due, at least in part, to the development of an acquired immune response as frogs approach adult size, for example, an increased production of lymphocytes (McMahon et al., 2014; Voyles, Rosenblum, & Berger, 2011). It is also possible that the development of a mature skin microbiome contributes to host recovery from high levels of *Bd* infection. As discussed above, a possible interpretation of our microbiome data is that post-metamorphic frogs begin with a relatively simple community of skin microbes and a higher level of microbiome diversity develops with age. Under this interpretation, the growing diversity of skin microbes could be providing the host with increased defence against *Bd* growth, leading to the declines in infection intensity we observed. Further research is needed to determine the mechanism underlying this negative correlation between infection intensity and size.

4.8 | Implications for the development of probiotic treatments

As emerging infectious diseases increasingly pose a threat to biodiversity across several wildlife systems, the use of probiotic treatments has emerged as a promising conservation strategy to aid in the recovery of threatened species. This study highlights both the promises and the challenges of efforts to develop bioaugmentation interventions to protect vulnerable amphibian species from the devastation of *Bd*. While *Janthinobacterium lividum* has garnered the most attention as an effective antifungal bacteria (Harris et al., 2009; Kueneman, Woodhams, Treuren, et al., 2016; Muletz et al., 2012), our *Bd* inhibition experiment from field-derived bacterial isolates demonstrates that there are numerous bacteria capable of inhibiting *Bd*—some of them even more effectively than *J. lividum*. All nine bacterial isolates included in this study significantly inhibited the growth of *Bd* in vitro (although their effects in vivo have yet to be assessed); this is promising for the development of probiotic treatments, since many trials using a wide range of bacterial taxa will likely be needed to identify a species that can persist on host skin long enough to alter infection outcomes in the long term (Bletz et al., 2013). Further research is needed to assess the inhibitory properties of these isolates in vivo.

However, the strong interactions we observed between *Bd* and the *R. sierrae* skin microbiome suggest that finding a bacterial species capable of persisting at elevated abundance on host skin may be difficult. The skin microbiome of “High ZE” frogs was strikingly different from “Low ZE” frogs, suggesting that *Bd* may exert a strong influence on community structure and species composition among “High ZE” frogs. If this is the case, then it may be difficult to meaningfully alter the skin microbiome of infected *R. sierrae* in the wild. In our study, the relative abundance of bacteria in the order Burkholderiales increased significantly among “High ZE” frogs, while the relative abundances of virtually all other dominant bacterial taxa decreased. If *Bd* often suppresses skin bacterial diversity as strongly as in *R. sierrae*, then it may be difficult to augment the abundance of mutualistic bacteria, particularly in the long term. In addition, recent research suggests that taxonomically diverse assemblages of probiotic bacteria may be more effective at combating *Bd* than individual bacterial isolates (Antwis & Harrison, 2018; Piovia-Scott et al., 2017). We suggest that efforts to develop probiotic treatments should focus on assemblages of bacterial taxa that are found at high abundances in some individuals in a population, since the microbiome of those individuals may represent an alternative stable community structure (Beisner, Haydon, & Cuddington, 2003). If bioaugmentation experiments aim to mimic these alternative community structures, target bacteria may stand a better chance of persisting at elevated abundances in treated frogs. We also suggest that bioaugmentation efforts should focus on the ability of candidate bacteria to persist on hosts in the long

term—even though such candidates will likely be elusive—since long-term persistence will be critical to successfully changing infection outcomes in threatened populations and species.

ACKNOWLEDGEMENTS

We thank May Ma, Niquo Ceberio, Natalie Greer and Erica Cartano for their assistance in the laboratory and Neil Kauffman and Kai Atkinson for their assistance in the field. We thank Cherie Briggs and Mary Toothman for providing the *Bd* standards. We also thank the U.S. Forest Service (especially Sarah Muskopf and Jann Williams), U.S. Fish and Wildlife Service and California Department of Fish and Wildlife for permits and valuable feedback. This research was supported primarily by funding from the U.S. Forest Service Southern Nevada Public Lands Management Act Program (Grant #13-DG-11272170-002). Additional funding was provided by the National Science Foundation (V. T. Vredenburg; DEB-11202283, Belmont Forum project NSF 1633948), the San Francisco State University Biology Department, California State University Program for Education and Research in Biotechnology and the American Museum of Natural History.

DATA ACCESSIBILITY

All data used in this study have been archived in the Dryad Digital Repository (https://doi.org/10.5061/dryad.8b83gn8).

AUTHOR CONTRIBUTIONS

S.E., V.T.V. and R.A.K. conceived the study and conducted fieldwork. S.E. performed laboratory work, analysed the data and wrote the manuscript. W.S. conceived and performed *Bd* inhibition assays. S.E., V.T.V., R.A.K., A.S. and W.S. edited and approved the final manuscript.

ORCID

Silas Ellison https://orcid.org/0000-0002-7698-4013
Roland A. Knapp https://orcid.org/0000-0002-1954-2745
Vance T. Vredenburg https://orcid.org/0000-0002-9682-1190

REFERENCES

Altschul, S. F., Gish, W., Miller, W., Myers, E. W., & Lipman, D. J. (1990). Basic local alignment search tool. *Journal of Molecular Biology*, *215*(3), 403–410. https://doi.org/10.1016/S0022-2836(05)80360-2

Antwis, R. E., & Harrison, X. A. (2018). Probiotic consortia are not uniformly effective against different amphibian chytrid pathogen isolates. *Molecular Ecology*, *27*(2), 577–589. https://doi.org/10.1111/mec.14456

Bailey, L. L., Kendall, W. L., Church, D. R., & Wilbur, H. M. (2004). Estimating survival and breeding probability for pond-breeding amphibians: A modified robust design. *Ecology*, *85*(9), 2456–2466. https://doi.org/10.1890/03-0539

Balzola, F., Bernstein, C., & Ho, G. T. (2011). A pyrosequencing study in twins shows that gastrointestinal microbial profiles vary with inflammatory bowel disease phenotypes: Commentary. *Inflammatory Bowel Disease Monitor*, *11*(4), 166. https://doi.org/10.1053/j.gastro.2010.08.049

Bates, K. A., Clare, F. C., O'Hanlon, S., Bosch, J., Brookes, L., Hopkins, K., … Harrison, X. A. (2018). Amphibian chytridiomycosis outbreak dynamics are linked with host skin bacterial community structure. *Nature Communications*, *9*(1), 1–11. https://doi.org/10.1038/s41467-018-02967-w

Becker, M. H., Harris, R. N., Minbiole, K. P. C., Schwantes, C. R., Rollins-Smith, L. A., Reinert, L. K., … Gratwicke, B. (2011). Towards a better understanding of the use of probiotics for preventing chytridiomycosis in Panamanian golden frogs. *EcoHealth*, *8*(4), 501–506. https://doi.org/10.1007/s10393-012-0743-0

Beisner, B. E., Haydon, D. T., & Cuddington, K. (2003). Alternative stable states in ecology. *Frontiers in Ecology and the Environment*, *1*(7), 376–382. https://doi.org/10.1890/1540-9295(2003)001[0376:ASSIE]2.0.CO;2

Bell, S. C., Alford, R. A., Garland, S., Padilla, G., & Thomas, A. D. (2013). Screening bacterial metabolites for inhibitory effects against *Batrachochytrium dendrobatidis* using a spectrophotometric assay. *Diseases of Aquatic Organisms*, *103*(1), 77–85. https://doi.org/10.3354/dao02560

Bletz, M. C., Loudon, A. H., Becker, M. H., Bell, S. C., Woodhams, D. C., Minbiole, K. P. C., & Harris, R. N. (2013). Mitigating amphibian chytridiomycosis with bioaugmentation: Characteristics of effective probiotics and strategies for their selection and use. *Ecology Letters*, *16*, 807–820. https://doi.org/10.1111/ele.12099

Boyle, D. G., Boyle, D. B., Olsen, V., Morgan, J. A. T., & Hyatt, A. D. (2004). Rapid quantitative detection of chytridiomycosis (*Batrachochytrium dendrobatidis*) in amphibian samples using real-time Taqman PCR assay. *Diseases of Aquatic Organisms*, *60*(2), 141–148. https://doi.org/10.3354/dao060141

Briggs, C. J., Knapp, R. A., & Vredenburg, V. T. (2010). Enzootic and epizootic dynamics of the chytrid fungal pathogen of amphibians. *Proceedings of the National Academy of Sciences of the United States of America*, *107*(21), 9695–9700. https://doi.org/10.1073/pnas.0912886107

Caporaso, J. G., Bittinger, K., Bushman, F. D., DeSantis, T. Z., Andersen, G. L., & Knight, R. (2010). PyNAST: A flexible tool for aligning sequences to a template alignment. *Bioinformatics (Oxford, England)*, *26*(2), 266–267. https://doi.org/10.1093/bioinformatics/btp636

Caporaso, J. G., Kuczynski, J., Stombaugh, J., Bittinger, K., Bushman, F. D., Costello, E. K., … Knight, R. (2010). QIIME allows analysis of high-throughput community sequencing data. *Nature Methods*, *7*(5), 335–336. https://doi.org/10.1038/nmeth.f.303

Clarke, K. R., & Ainsworth, M. (1993). A method of linking multivariate community structure to environmental variables. *Marine Ecology Progress Series*, *92*(3), 205–219. https://doi.org/10.3354/meps092205

Costello, E. K., Stagaman, K., Dethlefsen, L., Bohannan, B. J. M., & Relman, D. A. (2012). The application of ecological theory toward an understanding of the human microbiome. *Science*, *336*(6086), 1255–1262. https://doi.org/10.1126/science.1224203

Culp, C. E., Falkinham, J., & Belden, L. K. (2007). Identification of the natural bacterial microflora on the skin of eastern newts, bullfrog tadpoles and redback salamanders. *Herpetologica*, *63*(1), 66–71. https://doi.org/10.1655/0018-0831(2007)63[66:IOTNBM]2.0.CO;2

Daszak, P., Cunningham, A., & Hyatt, A. (2000). Emerging infectious diseases of wildlife—Threats to biodiversity and human health. *Science*, *287*(5452), 443–449. https://doi.org/10.1126/science.287.5452.443

DeSantis, T. Z., Hugenholtz, P., Larsen, N., Rojas, M., Brodie, E. L., Keller, K., … Andersen, G. L. (2006). Greengenes, a chimera-checked 16S rRNA gene database and workbench compatible with ARB. *Applied*

and Environmental Microbiology, *72*(7), 5069–5072. https://doi.org/10.1128/AEM.03006-05

Edgar, R. C. (2010). Search and clustering orders of magnitude faster than BLAST. *Bioinformatics (Oxford, England)*, *26*(19), 2460–2461. https://doi.org/10.1093/bioinformatics/btq461

Elmqvist, T., Folke, C., Nystrom, M., Peterson, G., Bengtsson, J., Walker, B., & Norberg, J. (2003). Response diversity, ecosystem change, and resilience. *Frontiers in Ecology and the Environment*, *1*(9), 488–494. https://doi.org/10.2307/3868116

Flechas, S. V., Sarmiento, C., Cárdenas, M. E., Medina, E. M., Restrepo, S., & Amézquita, A. (2012). Surviving Chytridiomycosis: Differential anti-*Batrachochytrium dendrobatidis* activity in bacterial isolates from three lowland species of *Atelopus*. *PLoS ONE*, *7*(9), e44832. https://doi.org/10.1371/journal.pone.0044832

Harris, R. N., Brucker, R. M., Walke, J. B., Becker, M. H., Schwantes, C. R., Flaherty, D. C., … Minbiole, K. P. C. (2009). Skin microbes on frogs prevent morbidity and mortality caused by a lethal skin fungus. *The ISME Journal*, *3*(7), 818–824. https://doi.org/10.1038/ismej.2009.27

Huttenhower, C., Gevers, D., Knight, R., Abubucker, S., Badger, J. H., Chinwalla, A. T., … White, O. (2012). Structure, function and diversity of the healthy human microbiome. *Nature*, *486*(7402), 207–214. https://doi.org/10.1038/nature11234

Hyatt, A. D., Boyle, D. G., Olsen, V., Boyle, D. B., Berger, L., Obendorf, D., … Coiling, A. (2007). Diagnostic assays and sampling protocols for the detection of *Batrachochytrium dendrobatidis*. *Diseases of Aquatic Organisms*, *73*(3), 175–192. https://doi.org/10.3354/dao073175

Jani, A. J., & Briggs, C. J. (2014). The pathogen *Batrachochytrium dendrobatidis* disturbs the frog skin microbiome during a natural epidemic and experimental infection. *Proceedings of the National Academy of Sciences of the United States of America*, *111*(47), E5049–E5058. https://doi.org/10.1073/pnas.1412752111

Jani, A. J., Knapp, R. A., & Briggs, C. J. (2017). Epidemic and endemic pathogen dynamics correspond to distinct host population microbiomes at a landscape scale. *Proceedings of the Royal Society B: Biological Sciences*, *284*(1857), 20170944. https://doi.org/10.1098/rspb.2017.0944

Kinney, V. C., Heemeyer, J. L., Pessier, A. P., Lannoo, M. J., & Samples, F. (2011). Seasonal pattern of *Batrachochytrium dendrobatidis* infection and mortality in *Lithobates areolatus*: Affirmation of Vredenburg's "10,000 Zoospore Rule". *PLoS ONE*, *6*(3), e16708. https://doi.org/10.1371/journal.pone.0016708

Klindworth, A., Pruesse, E., Schweer, T., Peplies, J., Quast, C., Horn, M., & Glöckner, F. O. (2013). Evaluation of general 16S ribosomal RNA gene PCR primers for classical and next-generation sequencing-based diversity studies. *Nucleic Acids Research*, *41*(1), e1. https://doi.org/10.1093/nar/gks808

Kueneman, J. G., Parfrey, L. W., Woodhams, D. C., Archer, H. M., Knight, R., & McKenzie, V. J. (2013). The amphibian skin-associated microbiome across species, space and life history stages. *Molecular Ecology*, *23*, 1238–1250. https://doi.org/10.1111/mec.12510.

Kueneman, J., Weiss, S., & McKenzie, V. (2017). Composition of microeukaryotes on the skin of the Cascades frog (*Rana cascadae*) and patterns of correlation between skin microbes and *Batrachochytrium dendrobatidis*. *Frontiers in Microbiology*, *8*(December), 2350. https://doi.org/10.3389/FMICB.2017.02350.

Kueneman, J. G., Woodhams, D. C., Harris, R., Archer, H. M., Knight, R., & McKenzie, V. J. (2016). Probiotic treatment restores protection against lethal fungal infection lost during amphibian captivity. *Proceedings of the Royal Society of London B: Biological Sciences*, *283*(1839), 20161553. https://doi.org/10.1098/rspb.2016.1553

Kueneman, J. G., Woodhams, D. C., Treuren, W. V., Archer, H. M., Knight, R., & Mckenzie, V. J. (2016). Inhibitory bacteria reduce fungi on early life stages of endangered Colorado boreal toads (*Anaxyrus boreas*). *The ISME Journal*, *10*(4), 934–944. https://doi.org/10.1038/ismej.2015.168

Lauer, A., Simon, M. A., Banning, J. L., André, E., Duncan, K., & Harris, R. N. (2007). Common cutaneous bacteria from the eastern red-backed salamander can inhibit pathogenic fungi. *Copeia*, *2007*(3), 630–640. https://doi.org/10.1643/0045-8511(2007)2007[630:CCBFTE]2.0.CO;2

Levine, J. M., & Antonio, C. M. D. (1999). Elton revisited: A review of evidence linking diversity and invasibility. *Oikos*, *87*(1), 15–26.

Lozupone, C., & Knight, R. (2005). UniFrac: A new phylogenetic method for comparing microbial communities. *Applied and Environmental Microbiology*, *71*(12), 8228–8235. https://doi.org/10.1128/AEM.71.12.8228

Lozupone, C. A., Stombaugh, J. I., Gordon, J. I., Jansson, J. K., & Knight, R. (2012). Diversity, stability and resilience of the human gut microbiota. *Nature*, *489*(7415), 220–230. https://doi.org/10.1038/nature11550

McDonald, D., Price, M. N., Goodrich, J., Nawrocki, E. P., DeSantis, T. Z., Probst, A., … Hugenholtz, P. (2012). An improved Greengenes taxonomy with explicit ranks for ecological and evolutionary analyses of bacteria and archaea. *The ISME Journal*, *6*(3), 610–618. https://doi.org/10.1038/ismej.2011.139

McMahon, T. A., Sears, B. F., Venesky, M. D., Bessler, S. M., Brown, J. M., Deutsch, K., … Rohr, J. R. (2014). Amphibians acquire resistance to live and dead fungus overcoming fungal immunosuppression. *Nature*, *511*(7508), 224–227. https://doi.org/10.1038/nature13491

Muletz, C. R., Myers, J. M., Domangue, R. J., Herrick, J. B., & Harris, R. N. (2012). Soil bioaugmentation with amphibian cutaneous bacteria protects amphibian hosts from infection by *Batrachochytrium dendrobatidis*. *Biological Conservation*, *152*, 119–126. https://doi.org/10.1016/j.biocon.2012.03.022

Muletz-wolz, C. R., Almario, J. G., Barnett, S. E., Direnzo, G. V., Martel, A., Pasmans, F., … Ritchie, K. B. (2017). Inhibition of fungal pathogens across genotypes and temperatures by amphibian skin bacteria. *Frontiers in Microbiology 8*(August), 1–10. https://doi.org/10.3389/fmicb.2017.01551.

Ouellet, M., Mikaelian, I., Pauli, B. D., Rodrigue, J., & Green, D. M. (2005). Historical evidence of widespread chytrid infection in North American amphibian populations. *Conservation Biology*, *19*(5), 1431–1440. https://doi.org/10.1111/j.1523-1739.2005.00108.x

Piovia-Scott, J., Rejmanek, D., Woodhams, D. C., Worth, S. J., Kenny, H., McKenzie, V., … Foley, J. E. (2017). Greater species richness of bacterial skin symbionts better suppresses the amphibian fungal pathogen *Batrachochytrium dendrobatidis*. *Microbial Ecology*, *74*(1), 217–226. https://doi.org/10.1007/s00248-016-0916-4

Price, M. N., Dehal, P. S., & Arkin, A. P. (2010). FastTree 2–approximately maximum-likelihood trees for large alignments. *PLoS ONE*, *5*(3), e9490. https://doi.org/10.1371/journal.pone.0009490

Reasoner, D. J., & Geldreich, E. E. (1985). A new medium for the enumeration and subculture of bacteria from potable water. *Applied and Environmental Microbiology*, *49*(1), 1–7.

Tilg, H., & Kaser, A. (2011). Gut microbiome, obesity, and metabolic dysfunction. *J Clin Invest*, *121*(6), 2126–2132. https://doi.org/10.1172/JCI58109.2126

Turnbaugh, P. J., Hamady, M., Yatsunenko, T., Cantarel, B. L., Duncan, A., Ley, R. E., … Gordon, J. I. (2009). A core gut microbiome in obese and lean twins. *Nature*, *457*(7228), 480–484. https://doi.org/10.1038/nature07540

Vázquez-Baeza, Y., Pirrung, M., Gonzalez, A., & Knight, R. (2013). EMPeror: A tool for visualizing high-throughput microbial community data. *GigaScience*, *2*(16), 2–5.

Voyles, J., Rosenblum, E. B., & Berger, L. (2011). Interactions between *Batrachochytrium dendrobatidis* and its amphibian hosts: A review of pathogenesis and immunity. *Microbes and Infection*, *13*(1), 25–32. https://doi.org/10.1016/j.micinf.2010.09.015

Voyles, J., Vredenburg, V. T., Tunstall, T. S., Parker, J. M., Briggs, C. J., & Rosenblum, E. B. (2012). Pathophysiology in mountain yellow-legged frogs (*Rana muscosa*) during a chytridiomycosis outbreak. *PLoS ONE*, *7*(4), e35374. https://doi.org/10.1371/journal.pone.0035374

Voyles, J., Young, S., Berger, L., Campbell, C., Voyles, W. F., Dinudom, A., … Speare, R. (2009). Pathogenesis of chytridiomycosis, a cause of catastrophic amphibian declines. *Science*, *326*(5952), 582–585. https://doi.org/10.1126/science.1176765

Vredenburg, V. T. (2004). Reversing introduced species effects: Experimental removal of introduced fish leads to rapid recovery of a declining frog. *Proceedings of the National Academy of Sciences of the United States of America*, *101*(20), 7646–7650. https://doi.org/10.1073/pnas.0402321101

Vredenburg, V. T., Bingham, R., Knapp, R., Morgan, J. A. T., Moritz, C., & Wake, D. (2007). Concordant molecular and phenotypic data delineate new taxonomy and conservation priorities for the endangered mountain yellow-legged frog. *Journal of Zoology*, *271*(4), 361–374. https://doi.org/10.1111/j.1469-7998.2006.00258.x

Vredenburg, V. T., Knapp, R. A., Tunstall, T. S., & Briggs, C. J. (2010). Dynamics of an emerging disease drive large-scale amphibian population extinctions. *Proceedings of the National Academy of Sciences of the United States of America*, *107*(21), 9689–9694. https://doi.org/10.1073/pnas.0914111107

Wake, D. B., & Vredenburg, V. T. (2008). Are we in the midst of the sixth mass extinction? A view from the world of amphibians. *Proceedings of the National Academy of Sciences of the United States of America*, *105*, 11466–11473. https://doi.org/10.1073/pnas.0801921105

Wang, Q., Garrity, G. M., Tiedje, J. M., & Cole, J. R. (2007). Naive Bayesian classifier for rapid assignment of rRNA sequences into the new bacterial taxonomy. *Applied and Environmental Microbiology*, *73*(16), 5261–5267. https://doi.org/10.1128/AEM.00062-07

Werner, J. J., Koren, O., Hugenholtz, P., DeSantis, T. Z., Walters, W. A., Caporaso, J. G., … Ley, R. E. (2012). Impact of training sets on classification of high-throughput bacterial 16s rRNA gene surveys. *The ISME Journal*, *6*(1), 94–103. https://doi.org/10.1038/ismej.2011.82

Woodhams, D. C., Brandt, H., Baumgartner, S., Kielgast, J., Küpfer, E., Tobler, U., … McKenzie, V. (2014). Interacting symbionts and immunity in the amphibian skin mucosome predict disease risk and probiotic effectiveness. *PLoS ONE*, *9*(4), e96375. https://doi.org/10.1371/journal.pone.0096375

SUPPORTING INFORMATION

Additional supporting information may be found online in the Supporting Information section at the end of the article.

How to cite this article: Ellison S, Knapp RA, Sparagon W, Swei A, Vredenburg VT. Reduced skin bacterial diversity correlates with increased pathogen infection intensity in an endangered amphibian host. *Mol Ecol.* 2018;00:1–14. https://doi.org/10.1111/mec.14964